NUCLEAR SCIENCE AND ENGINEERING: 99, 91-98 (1988)

Stability Analysis of Synthetic Acceleration Methods with Anisotropic Scattering

Dimitris Valougeorgis

Virginia Polytechnic Institute and State University
Center for Transport Theory and Mathematical Physics
Department of Mathematics, Blacksburg, Virginia 24061

Michael Williams

Virginia Polytechnic Institute and State University
Department of Mathematics, Blacksburg, Virginia 24061

and

Edward W. Larsen

The University of Michigan, Department of Nuclear Engineering
Ann Arbor, Michigan 48109

Received May 15, 1987
Accepted November 4, 1987

Abstract — *A study of the spectral radius for the continuous form of the source iteration, diffusion synthetic acceleration, and various P_L acceleration methods ($L \geq 1$) for anisotropically scattering neutron transport is carried out via a Fourier stability analysis. The purpose of the study is to determine which acceleration scheme is optimum. The problem is formulated as a matrix eigenvalue problem with, in general, $N + 1$ iteration eigenvalues ω where N denotes the degree of anisotropy. The P_1 acceleration method is determined as the most efficient P_L approach for the cases of linearly and quadratically anisotropic scattering.*

I. INTRODUCTION

The diffusion synthetic acceleration[1-6] (DSA) method has been extensively used to accelerate the slow convergence of the source iteration (SI) method for neutron transport problems in optically thick regions with scattering ratios c near unity. Stability difficulties of early versions of the DSA method have, to some extent, been resolved[4,5] by developing difference schemes of the diffusion equation that are consistent with the difference schemes of the transport equation. Very recently, Miller and Larsen[7] studied the spectral radius of general P_L acceleration methods and found that for problems with isotropic scattering, DSA (or P_1 acceleration) is the optimum P_L approach. The general case of anisotropic scattering was first considered by Morel.[8] He found experimentally that a P_1 acceleration scheme, which now is not equivalent to DSA, is superior to DSA.

In this paper, we study the effectiveness of P_L acceleration of the iteration process for solving the transport equation with two coefficients of anisotropy and $L \leq 3$. Our study is restricted to the analytic transport equation with no angular or spatial discretization. Our approach is based on a Fourier analysis to determine the spectral radius of the iteration operator. Without a doubt, the use of the infinite medium constant cross-section problem as the model problem for the Fourier analysis is highly idealized. However, previous experience with DSA indicates predictions of the spectral radius that are quite close to the numerical convergence rates of more realistic problems. For

example, our present results for the linearly and quadratically anisotropic scattering cases provide theoretical evidence of the empirical results of Morel.[8] It is important to note that the present Fourier analysis leads in general to $N + 1$ distinct eigenvalues and eigenvectors, where N is the order of anisotropy. The number of accelerated moments plays an important role in the behavior of these eigenvalues as a function of the Fourier frequency.

We begin our analysis in Sec. II with a study of the SI method. We continue in Sec. III with the development of a P_L acceleration method assuming two degrees of scattering anisotropy. In addition, we present numerical results for the theoretical convergence rates of certain P_L acceleration methods. Section IV contains results and general remarks about the performance of P_L acceleration schemes in all Cartesian geometries. Finally, in Sec. V, we give a brief summary and conclusions.

II. SI METHOD

The SI method can be described by the equations

$$\mu \frac{\partial \psi^{(l+1/2)}}{\partial x} + \psi^{(l+1/2)}(x,\mu) = c\sum_{n=0}^{N} (2n+1) f_n P_n(\mu) \varphi_n^{(l)}(x) + s(x) \quad (1)$$

and

$$\varphi_n^{(l+1)}(x) = \frac{1}{2}\int_{-1}^{1} P_n(\mu)\psi^{(l+1/2)}(x,\mu)\, d\mu \ , \quad (2)$$

where

$\psi(x,\mu)$ = particle density

f_n = n'th coefficient of anisotropy

$P_n(\mu)$ = n'th Legendre polynomial

$\varphi_n(x)$ = n'th Legendre moment of $\psi(x,\mu)$ defined by Eq. (2)

l = iteration index.

To determine the spectral radius of the SI scheme, we define

$$\Psi^{(l+1/2)}(x,\mu) = \psi^{(l+1/2)}(x,\mu) - \psi^{(l-1/2)}(x,\mu) \quad (3a)$$

and

$$\Phi^{(l+1)} = \varphi^{(l+1)}(x) - \varphi^{(l)}(x) \ , \quad (3b)$$

and apply a separation of variable Fourier mode solution to the equations

$$\mu \frac{\partial \Psi^{(l+1/2)}}{\partial x} + \Psi^{(l+1/2)}(x,\mu) = c\sum_{n=0}^{N} (2n+1) f_n P_n(\mu) \Phi_n^{(l)}(x) \quad (4)$$

and

$$\Phi_n^{(l+1)}(x) = \frac{1}{2}\int_{-1}^{1} P_n(\mu)\Psi^{(l+1/2)}(x,\mu)\, d\mu \ . \quad (5)$$

These equations are obtained by subtracting Eqs. (1) and (2) for successive iterates. We use the Fourier mode ansatz:

$$\Psi^{(l+1/2)}(x,\mu) = \omega^l g(\mu)\exp(i\lambda x) \ , \quad (i = \sqrt{-1}) \quad (6)$$

and

$$\Phi_n^{(l)}(x) = \omega^l b_n \exp(i\lambda x) \ , \quad (7)$$

where ω is the eigenvalue corresponding to the Fourier frequency λ. Substituting Eqs. (6) and (7) into Eqs. (4) and (5), we obtain

$$g(\mu) = \frac{c}{1 + i\lambda\mu}\sum_{n=0}^{N} (2n+1) f_n P_n(\mu) b_n \quad (8)$$

and

$$\omega b_n = \sum_{m=0}^{N}\left[\frac{1}{2} c(2m+1) f_m \times \int_{-1}^{1} \frac{P_n(\mu)P_m(\mu)}{1 + i\lambda\mu}\, d\mu\right] b_m \ , \quad 0 \le n \le N \ . \quad (9)$$

Hence, if we define

$$A_{nm}(\lambda) = \frac{c}{2}(2m+1) f_m \times \int_{-1}^{1} \frac{P_n(\mu)P_m(\mu)}{1 + i\lambda\mu}\, d\mu \ , \quad 0 \le n, m \le N \ , \quad (10)$$

then we obtain the matrix eigenvalue problem

$$\omega b_n = \sum_{m=0}^{N} A_{nm} b_m \ , \quad 0 \le n \le N \ . \quad (11)$$

By setting $\lambda = 0$, we can easily deduce from Eqs. (10) and (11) that $\omega_i(0) = cf_i$, $0 \le i \le N$. Note that, in general, there are $N + 1$ distinct eigenvalues and eigenvectors. To obtain the spectral radius

$$\rho = \max_{0 \le i \le N} \sup_{\lambda} |\omega_i(\lambda)| \quad (12)$$

of the iteration map, an upper bound for $|\omega_i|$ as a function of the parameter λ must be determined.

To demonstrate some explicit results, we consider here the special case of linearly anisotropic scattering. We find

$$\mathbf{A}(\lambda) = c\begin{bmatrix} \Lambda & -3if_1(1-\Lambda)/\lambda \\ -i(1-\Lambda)/\lambda & 3f_1(1-\Lambda)/\lambda^2 \end{bmatrix} \ , \quad (13)$$

where

$$\Lambda = \tan^{-1}(\lambda)/\lambda \ , \tag{14}$$

and the expressions for the two eigenvalues are

$$\omega_{1,2} = \frac{c}{2}\left\{\Lambda + 3f_1\frac{1-\Lambda}{\lambda^2} \pm \left[\Lambda^2 + 3f_1\frac{1-\Lambda}{\lambda^2} \times \left(2\Lambda + 3f_1\frac{1-\Lambda}{\lambda^2} - 4\right)\right]^{1/2}\right\} . \tag{15}$$

Plots of ω versus λ for the SI method are given in Fig. 1 for $c = 1$ and for $f_1 = 0$ (isotropic scattering) and $f_1 = \frac{1}{3}$. Both "anisotropic" eigenvalues are real for $0 \le \lambda \le 1.93$ and are complex conjugates for $\lambda \ge 1.94$. In Fig. 1, we plot the absolute value of λ for $\lambda \ge 1.94$. The two eigenvalues corresponding to the anisotropic case are less than the isotropic eigenvalue for all values of $\lambda > 0$. Since for a finite system the flat $\lambda = 0$ mode cannot be present, we may argue that the convergence of the linearly anisotropic problem should be slightly faster than for the isotropic problem. However, for the model problem under consideration, we find the absolute maximum value of all ω, which occurs at $\lambda = 0$, to be independent of f_1 and equal to c. Hence, for c (arbitrarily) close to unity, the SI method will converge (arbitrarily) slowly.

III. THE ANISOTROPIC P_L ACCELERATION METHOD

III.A. Formulation of the Scheme and Stability Analysis

For simplicity we restrict our study to the transport equation with quadratically anisotropic scattering. Williams[9] has derived a synthetic acceleration scheme with highly forward-peaked scattering. However, because his derivation was somewhat peripheral to the main purpose of this paper, we present again a similar P_L acceleration analysis.

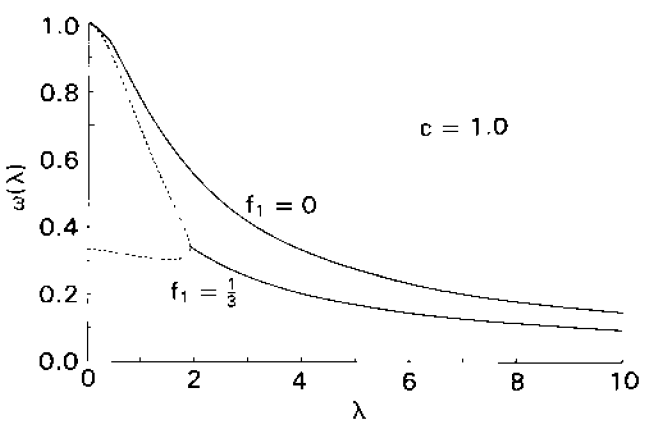

Fig. 1. Plots of ω versus λ for the SI method with isotropic scattering (upper curve) and linearly anisotropic scattering (lower curves).

The form of the equation under consideration here is

$$\mu\frac{\partial\psi^{(l+1/2)}}{\partial x} + \psi^{(l+1/2)}(x,\mu) = c[f_0\varphi_0^{(l)}(x) + 3f_1P_1(\mu)\varphi_1^{(l)}(x) + 5f_2P_2(\mu)\varphi_2^{(l)}(x)] + s(x) \ , \tag{16}$$

where the terms are as defined earlier. Formulating the desired acceleration scheme, we take the first $K+1$ Legendre's moments of Eq. (16) to obtain the set of equations

$$\frac{k+1}{2k+1}\frac{d\varphi_{k+1}^{(l+1/2)}}{dx} + \frac{k}{2k+1}\frac{d\varphi_{k-1}^{(l+1/2)}}{dx} + \varphi_k^{(l+1/2)} = cf_k\varphi_k + \delta_{k0}s \ , \quad k = 0,1,\ldots,K \ , \tag{17}$$

and we now define the acceleration equations as

$$\frac{k+1}{2k+1}\frac{d\varphi_{k+1}^{(l+1)}}{dx} + \frac{k}{2k+1}\frac{d\varphi_{k-1}^{(l+1)}}{dx} + (1-cf_k)\varphi_k^{(l+1)} = \delta_{k0}s \ , \quad k = 0,1,\ldots,K-1 \tag{18a}$$

and

$$\frac{K}{2K+1}\frac{d\varphi_{k-1}^{(l+1)}}{dx} + (1-cf_K)\varphi_K^{(l+1)} = -\frac{K+1}{2K+1}\frac{d\varphi_{K+1}^{(l+1/2)}}{dx} \ , \tag{18b}$$

where $f_k = 0$ for $k > 2$. Subtracting Eqs. (16) and (18) for successive values of l, we obtain the equations

$$\mu\frac{\partial\Psi^{(l+1/2)}}{\partial x} + \Psi^{(l+1/2)}(x,\mu) = c[f_0\Phi_0^{(l)}(x) + 3f_1P_1(\mu)\Phi_1^{(l)}(x) + 5f_2P_2(\mu)\Phi_2^{(l)}(x)] \ , \tag{19}$$

$$\frac{k+1}{2k+1}\frac{d\Phi_{k+1}^{(l+1)}}{dx} + \frac{k}{2k+1}\frac{d\Phi_{k-1}^{(l+1)}}{dx} + (1-cf_k)\Phi_k^{(l+1)} = 0 \ , \quad k = 0,1,\ldots,K-1 \ , \tag{20a}$$

and

$$\frac{K}{2K+1}\frac{d\Phi_{K-1}^{(l+1)}}{dx} + (1-cf_K)\Phi_K^{(l+1)} = -\frac{K+1}{2K+1}\frac{d\Phi_{K+1}^{(l+1/2)}}{dx} \ , \tag{20b}$$

which are amenable to Fourier analysis. Proceeding as before, Eqs. (6) and (7) are introduced into Eq. (19) to find

$$g(\mu) = \frac{c}{1+i\lambda\mu}\sum_{n=0}^{2}(2n+1)f_nP_n(\mu)b_n \tag{21}$$

and into Eqs. (20) to obtain the vector equation

$$\omega \mathbf{D} \boldsymbol{b} = -\frac{K+1}{2K+1} i\lambda \boldsymbol{V} G_{K+1} , \tag{22}$$

where

$$\mathbf{D} = \begin{bmatrix} 1-cf_0 & i\lambda & 0 & 0 & \cdots & & 0 \\ i\lambda/3 & 1-cf_1 & 2i\lambda/3 & 0 & & & \vdots \\ 0 & 2i\lambda/5 & 1-cf_2 & 3i\lambda/5 & & & \\ 0 & 0 & 3i\lambda/7 & 1 & & & \\ \vdots & & & ki\lambda/(2k+1) & 1 & (k+1)i\lambda/(2k+1) & 0 \\ \vdots & & & & & & \\ 0 & \cdots & & & 0 & Ki\lambda/(2K+1) & 1 \end{bmatrix} ,$$

with $k = 0,1,\ldots,K$; $\boldsymbol{b}^T = (b_0, b_1, \ldots, b_K)$ and $\boldsymbol{V}^T = (0,0,\ldots,0,1)$ are two constant $(K+1)$ vectors; and

$$G_{K+1} = \frac{1}{2}\int_{-1}^{1} P_{K+1}(\mu) g(\mu)\, d\mu .$$

We now recast the expression for G_{K+1} into a more convenient form. Introducing Eq. (21) for $g(\mu)$, we obtain

$$G_{K+1} = \boldsymbol{F}\boldsymbol{b} , \tag{23}$$

where $\boldsymbol{F}$ is a row vector with components

$$F_n(\lambda) = cf_n \frac{2n+1}{2}\int_{-1}^{1} \frac{P_{K+1}(\mu)P_n(\mu)}{1+i\lambda\mu}\, d\mu ,$$

$$0 \le n \le K ,$$

where $F_n = 0$ for $n \ge 3$ because $f_n = 0$ for $n \ge 3$. Equation (22) can now be written as

$$\omega \boldsymbol{b} = \mathbf{A}\boldsymbol{b} , \tag{24}$$

with

$$\mathbf{A} = -\frac{K+1}{2K+1} i\lambda \mathbf{D}^{-1}\boldsymbol{V}\boldsymbol{F} . \tag{25}$$

It is obvious that this is an eigenvalue problem where ω are the eigenvalues of $\mathbf{A}$ and $\boldsymbol{b}$ the corresponding eigenvectors. However, we note that according to Eq. (25), $\mathbf{A}$ is the product of a column vector times a row vector, and because of that its rank is equal to unity. Hence, we obtain one dominant eigenvalue while the K remaining eigenvalues are identically equal to zero. In fact, by multiplying both sides of the vector [Eq. (24)] by $\boldsymbol{F}$, we deduce the following scalar equation:

$$\omega = -\frac{K+1}{2K+1} i\lambda \boldsymbol{F}\mathbf{D}^{-1}\boldsymbol{V} . \tag{26}$$

We conclude that in general a P_L acceleration scheme with $L \ge N$, where N denotes the degree of anisotropy, sets N of its $N+1$ eigenvalues equal to zero. Thus, study of the one nonzero eigenvalue is sufficient to obtain the convergence rate of the acceleration scheme. On the other hand, the choice of $L < N$ is reasonable since from a computational point of view it is desirable to solve a small system of P_L equations. In the following section, we evaluate the computational effectiveness of different P_L acceleration methods.

III.B. The Spectral Radius of Certain P_L Acceleration Algorithms

In this section, we develop closed form expressions for the eigenvalues of certain orders of P_L acceleration for the worst case of $c = 1.0$, and we then numerically solve these equations. We start our analysis with the evaluation of the convergence rate of the classical DSA scheme in the case of quadratically anisotropic scattering. The DSA method for the analytic transport equation is now described by Eq. (16) coupled to the diffusion equation:

$$\frac{1}{3}\frac{d^2\varphi_0^{(l+1)}}{dx^2} + (1-c)(1-cf_1)\varphi_0^{(l+1)} = -\frac{2}{3}\frac{d^2\varphi_0^{(l+1/2)}}{dx^2} , \tag{27}$$

while the first and second moments of the angular flux

$$\varphi_1^{(l+1)}(x) = \frac{1}{2}\int_{-1}^{1} P_1(\mu)\psi^{(l+1/2)}(x,\mu)\, d\mu \tag{28a}$$

and

$$\varphi_2^{(l+1)}(x) = \frac{1}{2}\int_{-1}^{1} P_2(\mu)\psi^{(l+1/2)}(x,\mu)\, d\mu , \tag{28b}$$

respectively, are not accelerated. Performing the same Fourier stability analysis on this method as we applied in the P_L acceleration method in Sec. III.A, we obtain $\omega_1 = 0$ and

$$\omega_{2,3} = \frac{1}{2}\left[\beta \pm (\beta^2 - 4\gamma)^{1/2}\right] , \tag{29}$$

where

$$\beta = \Lambda - \frac{3}{\lambda^2}(1-\Lambda)(1-f_1) + \frac{5}{4}f_2 \times \left[\frac{9}{\lambda^2}\left(\frac{1}{3} - \frac{1-\Lambda}{\lambda^2}\right) - \frac{6}{\lambda^2}(1-\Lambda) + \Lambda\right] \quad (30a)$$

and

$$\gamma = \frac{15}{4}f_1 f_2 \frac{1}{\lambda^2}\left[\left[\Lambda - \frac{3}{\lambda^2}(1-\Lambda)\right]^2 + (1-\Lambda) \times \left[\frac{9}{\lambda^2}\left(\frac{1}{3} - \frac{1-\Lambda}{\lambda^2}\right) - \frac{6}{\lambda^2}(1-\Lambda) + \Lambda\right]\right], \quad (30b)$$

with Λ defined in Eq. (14). From Eq. (29) it is easy to show that as λ approaches zero $\omega_2 = f_1$ and $\omega_3 = f_2$.

Next we consider the P_1 acceleration scheme, which is described by Eq. (16) and the acceleration equations

$$\frac{d\varphi_1^{(l+1)}}{dx} + (1-c)\varphi_0^{(l+1)} = 0 \quad (31a)$$

and

$$\frac{1}{3}\frac{d\varphi_0^{(l+1)}}{dx} + (1-cf_1)\varphi_1^{(l+1)} = -\frac{2}{3}\frac{d\varphi_2^{(l+1/2)}}{dx} \quad (31b)$$

and Eq. (28b). A similar Fourier analysis yields $\omega_1 = \omega_2 = 0$ and

$$\omega_3 = \left[\Lambda - \frac{3}{\lambda^2}(1-\Lambda)\right]\left(1 + \frac{5}{4}f_2\right) + \frac{45}{4}f_2\frac{1}{\lambda^2}\left(\frac{1}{3} - \frac{1-\Lambda}{\lambda^2}\right). \quad (32)$$

The last expression for the nonzero eigenvalue ($c = 1.0$) is independent of f_1, and $\omega_3 = f_2$ when $\lambda = 0$.

Finally, we consider P_L acceleration methods with $L = 2$ and 3. The formulation and stability analysis of these acceleration schemes can easily be deduced from Sec. III.A. The eigenvalues for these methods, which are obtained directly from Eqs. (24) and (26), are $\omega_1 = \omega_2 = 0$ and

$$\omega_3 = -\frac{3}{5(1-f_2)}\left\{3(1-\Lambda)\left(1 + \frac{5}{4}f_2\right) - 5\left(\frac{1}{3} - \frac{1-\Lambda}{\lambda^2}\right)\left(1 + \frac{7}{2}f_2\right) + \frac{75}{4}f_2\left[\frac{1}{5} - \frac{1}{\lambda^2}\left(\frac{1}{3}\frac{1-\Lambda}{\lambda^2}\right)\right]\right\}, \quad (33)$$

for P_2 acceleration, and $\omega_1 = \omega_2 = \omega_3 = 0$ and

$$\omega_4 = \frac{3\lambda^2}{9\lambda^2 + 35(1-f_2)} \times \left\{3\Lambda\left(1 + \frac{5}{4}f_2\right) - \frac{15}{\lambda^2}(1-\Lambda)\left(2 + \frac{13}{4}f_2\right) + \frac{5}{\lambda^2}\left(\frac{1}{3} - \frac{1-\Lambda}{\lambda^2}\right)\left(7 + \frac{125}{4}f_2\right) - \frac{525}{4}f_2\frac{1}{\lambda^2}\left[\frac{1}{5} - \frac{1}{\lambda^2}\left(\frac{1}{3} - \frac{1-\Lambda}{\lambda^2}\right)\right]\right\} \quad (34)$$

for P_3 acceleration. Both Eqs. (33) and (34) are independent of f_1.

We have numerically solved Eqs. (29), (32), (33), and (34), and Figs. 2, 3a, and 3b provide some insight into the behavior of ω as a function of λ. Table I contains the spectral radius for each of the four iteration-acceleration schemes under consideration. The inefficiency of the P_2 acceleration method is easily observed. In fact, this algorithm becomes unstable and nonconvergent when $f_2 \neq 0$. It seems that the historically bad performance of the even order P_L approximations[10] becomes even worse in the case of highly anisotropic scattering.

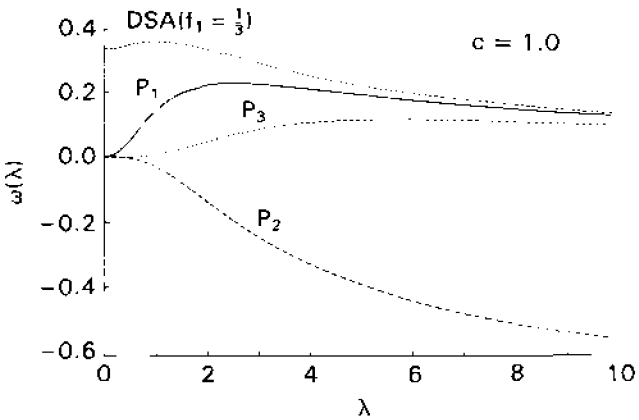

Fig. 2. Plots of ω versus λ for various orders of P_L acceleration with linearly anisotropic scattering.

TABLE I

Spectral Radius of Anisotropic Synthetic Acceleration Methods

Acceleration Method	f_1	0.0	$\frac{1}{3}$		
	f_2	0.0	0.0	0.2	0.4
DSA		0.2247	0.3562	0.4140	0.4972
P_1		0.2247	0.2247	0.3147	0.4261
P_2		0.8	0.8	1.25	2.0
P_3		0.1108	0.1108	0.1445	0.1806

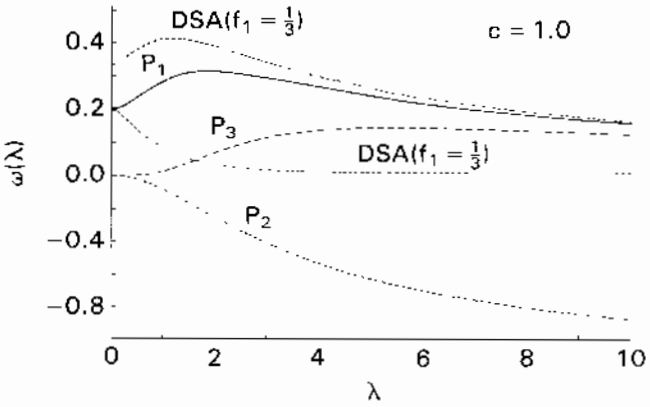

Fig. 3a. Plots of ω versus λ for various orders of P_l acceleration with quadratically anisotropic scattering, $f_2 = 0.2$.

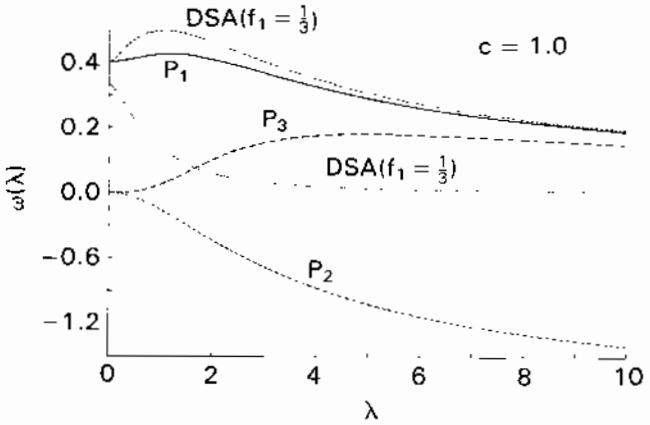

Fig. 3b. Plots of ω versus λ for various orders of P_L acceleration with quadratically anisotropic scattering, $f_2 = 0.4$.

In Fig. 2, we show the eigenvalues for various orders of P_L acceleration with linearly anisotropic scattering. By setting $f_2 = 0$, Eqs. (32), (33), and (34), which are independent of the first degree of anisotropy, reduce to the equivalent expressions for the case of isotropic scattering. Hence, we conclude that the effectiveness of the linearly anisotropic P_L acceleration with $L = 1,2,3$ remains identical to the effectiveness of P_L acceleration observed in isotropic scattering. The only exception is DSA, which now is not equivalent to P_1 acceleration and has a spectral radius that is a function of f_1 and equal to 0.3562 for $f_1 = \frac{1}{3}$ (worst case). The reduction in the error from one iteration to the next for the P_1 acceleration ($\rho = 0.2247$) is improved by a factor of 1.6, while the computational cost associated with the acceleration of the first moment is trivial.[8] This result provides a theoretical justification of the numerical work of Morel.[8] Following a simple calculation suggested by Miller and Larsen,[7] we find that two P_1 sweeps take 4 time units and reduce the error by a factor of 19.8, while a single P_3 sweep requires at least the same computational time and will reduce the error only by a factor of 9.02. Thus, we argue that for the case of linearly anisotropic scattering the P_1 acceleration method is the optimum technique.

In Figs. 3a and 3b, we present results for the more general case of quadratically anisotropic scattering with f_2 taking values in the set $\{0.2, 0.4\}$. The two curves associated with DSA correspond to the two nonzero eigenvalues. The performance of the standard DSA method is degraded with increasing anisotropy, with a spectral radius of ~ 0.5 for the worst case of $f_1 = \frac{1}{3}$ and $f_2 = 0.4$. The P_1 acceleration performs slightly better, while the P_3 acceleration is best. The spectral radius, going from the P_1 to P_3 acceleration, has been decreased by a factor of 2.36, but the computational effort of solving four coupled acceleration equations (or two coupled diffusion-type equations) has increased. Two P_1 sweeps reduce the error by a factor of 5.51, while at the same time a single P_3 sweep reduces the error by a factor of 5.54. Although the choice of the best P_L acceleration approach for quadratically anisotropic scattering is not as clear as for linear anisotropy, our results indicate that P_1 acceleration remains the optimum acceleration algorithm to solve realistic problems.

IV. P_L ACCELERATION IN ALL CARTESIAN GEOMETRIES

Now that we have selected the P_1 to be the optimum acceleration method for linearly and quadratically anisotropic scattering in slab geometry, we extend our study to the performance of the P_L acceleration in all Cartesian geometries. To avoid algebraic complexity, let us consider only the two-dimensional monoenergetic neutron transport equation with linear anisotropy. Then the standard SI sweep is described by

$$\left(\mu \frac{\partial}{\partial x} + \eta \frac{\partial}{\partial y} + 1\right) \psi^{(l+1/2)}(x,y,\mu,\eta) = c\,[f_0 \varphi_{00}^{(l)}(x,y) + 3f_1 P_1(\mu)\varphi_{10}^{(l)}(x,y) + 3f_1 P_1(\eta)\varphi_{01}^{(l)}(x,y)] \quad , \tag{35}$$

and the integral that defines the flux moments has been transformed to the corresponding integral over a disk

$$\varphi_{mn}^{(l+1)}(x,y) = L\,[P_m(\mu)P_n(\eta)\psi^{(l+1/2)}(x,y,\mu,\eta)] \quad . \tag{36}$$

The integral operator L is defined as

$$L = \frac{1}{2\pi}\int_{-1}^{1}\int_{-(1-\mu^2)^{1/2}}^{(1-\mu^2)^{1/2}} (1-\mu^2-\eta^2)^{-1/2}(\cdot)\,d\eta\,d\mu \ ,$$

and $P_m(\mu)$ and $P_n(\eta)$ are the m'th and n'th Legendre polynomials, respectively.

Formulating the P_1 acceleration scheme, we retain Eq. (35) and derive a set of synthetic equations by taking the zeroth and the two first moments (with respect to μ and η) of Eq. (35). To carry this out, Eq. (35) is multiplied first by $(1-\mu^2-\eta^2)^{-1/2}$ and then successively by $P_0(\mu)P_0(\eta)$, $P_1(\mu)P_0(\eta)$, and $P_0(\mu)P_1(\eta)$, yielding

$$\frac{\partial}{\partial x}\varphi_{10}^{(l+1)} + \frac{\partial}{\partial y}\varphi_{01}^{(l+1)} + (1-c)\varphi_{00}^{(l+1)} = 0 \ , \quad (37a)$$

$$\frac{1}{3}\frac{\partial}{\partial x}\varphi_{00}^{(l+1)} + (1-cf_1)\varphi_{10}^{(l+1)} = -\frac{2}{3}\frac{\partial}{\partial x}\varphi_{20}^{(l+1/2)} - \frac{\partial}{\partial y}\varphi_{11}^{(l+1/2)} \ , \quad (37b)$$

and

$$\frac{1}{3}\frac{\partial}{\partial y}\varphi_{00}^{(l+1)} + (1-cf_1)\varphi_{01}^{(l+1)} = -\frac{2}{3}\frac{\partial}{\partial y}\varphi_{02}^{(l+1/2)} - \frac{\partial}{\partial x}\varphi_{11}^{(l+1/2)} \ . \quad (37c)$$

We recast the transport and the acceleration equations into the following form:

$$\left(\mu\frac{\partial}{\partial x} + \eta\frac{\partial}{\partial y} + 1\right)\Psi^{(l+1/2)}(x,y,\mu,\eta) = c\,[f_0\Phi_{00}^{(l)}(x,y) + 3f_1P_1(\mu)\Phi_{10}^{(l)}(x,y) + 3f_1P_1(\eta)\Phi_{01}^{(l)}(x,y)] \ , \quad (38)$$

$$\frac{\partial}{\partial x}\Phi_{10}^{(l+1)} + \frac{\partial}{\partial y}\Phi_{01}^{(l+1)} + (1-c)\Phi_{00}^{(l+1)} = 0 \ , \quad (39a)$$

$$\frac{1}{3}\frac{\partial}{\partial x}\Phi_{00}^{(l+1)} + (1-cf_1)\Phi_{10}^{(l+1)} = -\frac{2}{3}\frac{\partial}{\partial x}\Phi_{20}^{(l+1/2)} - \frac{\partial}{\partial y}\Phi_{11}^{(l+1/2)} \ , \quad (39b)$$

and

$$\frac{1}{3}\frac{\partial}{\partial y}\Phi_{00}^{(l+1)} + (1-cf_1)\Phi_{01}^{(l+1)} = -\frac{2}{3}\frac{\partial}{\partial y}\Phi_{02}^{(l+1/2)} - \frac{\partial}{\partial x}\Phi_{11}^{(l+1/2)} \ , \quad (39c)$$

with

$$\Psi^{(l+1/2)}(x,y,\mu,\eta) = \psi^{(l+1/2)}(x,y,\mu,\eta) - \psi^{(l-1/2)}(x,y,\mu,\eta)$$

and

$$\Phi_{mn}^{(l+1)}(x,y) = \varphi_{mn}^{(l+1)} - \varphi_{mn}^{(l)} \ .$$

To determine the spectral radius of the P_1 scheme described by Eqs. (35) and (37), we introduce

$$\Psi^{(l+1/2)}(x,y,\mu,\eta) = \omega^l g(\mu,\eta)\exp[i\lambda(x\theta_x + y\theta_y)] \ , \quad (i=\sqrt{-1}) \quad (40a)$$

and

$$\Phi_{mn}^{(l)}(x,y) = \omega^l b_{mn}\exp[i\lambda(x\theta_x + y\theta_y)] \ , \quad (40b)$$

where $\lambda = \lambda(\theta_x,\theta_y)$ with $\theta_x^2 + \theta_y^2 = 1$. Substituting the ansatz, Eq. (40), into Eqs. (38) and (39) results in

$$g(\mu,\eta) = c\,\frac{b_{00} + 3f_1\mu b_{10} + 3f_1\eta b_{01}}{1 + i\lambda(\mu\theta_x + \eta\theta_y)} \quad (41)$$

and

$$\omega[i\lambda\theta_x b_{10} + i\lambda\theta_y b_{01} + (1-c)b_{00}] = 0 \ , \quad (42a)$$

$$\omega\left[\frac{i}{3}\lambda\theta_x b_{00} + (1-cf_1)b_{10}\right] = -i\frac{2}{3}\lambda\theta_x G_{20} - i\lambda\theta_y G_{11} \ , \quad (42b)$$

$$\omega\left[\frac{i}{3}\lambda\theta_y b_{00} + (1-cf_1)b_{01}\right] = -i\frac{2}{3}\lambda\theta_y G_{02} - i\lambda\theta_x G_{11} \ , \quad (42c)$$

respectively, where

$$G_{mn} = L[P_m(\mu)P_n(\eta)g(\mu,\eta)] \ .$$

Thus, we have a system of three equations, so, in general, for each λ there are three distinct eigenvalues and eigenvectors. After some routine manipulation, we obtain $\omega_1 = \omega_2 = 0$ and

$$\omega_3 = \frac{-3L[(\mu\theta_x + \eta\theta_y)^2 g(\mu,\eta)] + L[g(\mu,\eta)]}{1 + \frac{3}{\lambda^2}(1-c)(1-cf_1)} \ . \quad (43)$$

The integrals in the explicit expression for ω_3 can be evaluated analytically to yield

$$\omega_3 = c\,\frac{\left[1 - \frac{3}{\lambda^2}f_1(1-c)\right]\left[\left(1+\frac{3}{\lambda^2}\right)\Lambda - \frac{3}{\lambda^2}\right]}{1 + \frac{3}{\lambda^2}(1-c)(1-cf_1)} \ ; \quad (44)$$

finally, for $c = 1$ we get

$$\omega_3 = \Lambda - \frac{3}{\lambda^2}(1-\Lambda) \ , \quad (45)$$

where Λ is as defined earlier. The point to be stressed here is that Eq. (45) is independent of f_1 and is identical to Eq. (32) for $f_2 = 0$, which describes the one-dimensional P_1 acceleration method. Similar results can be obtained for various orders of P_L acceleration.

This analysis shows that plane wave solutions of the x,y or x,y,z exact transport equation must reduce to the solution of the slab geometry equation. Thus, for the analytic transport equation, P_L acceleration methods must perform equally well (or poorly) in all Cartesian geometries. We conclude that in multidimensional geometries the P_1 acceleration remains the preferred algorithm in order to obtain good acceleration in transport calculations with linear and quadratic anisotropy.

V. CONCLUSIONS

In this paper, we have developed a Fourier stability analysis to evaluate the convergence rates of the SI, DSA, and P_L acceleration methods in their continuous form for the case of anisotropic scattering. The problem is formulated as an eigenvalue problem with, in general, $N + 1$ iteration eigenvalues ω, where N denotes the degree of anisotropy. By studying various P_L acceleration schemes, we proved that the performance of the DSA method is degraded as the scattering becomes more forward peaked, but the DSA scheme is significantly improved if one accelerates both the zero and the first angular moments. In fact, we found, from an overall computational point of view, that this P_1 acceleration method is the most efficient P_L approach for the cases of linearly and quadratically anisotropic scattering in all Cartesian geometries. However, Table I shows that the spectral radius of the P_1 acceleration method also increases for increasing anisotropy. We note that for the worst case under consideration ($f_1 = \frac{1}{3}, f_2 = 0.4$) the P_1 and P_3 methods are competitive. Because of this, higher order acceleration schemes may be competitive when the scattering is more forward peaked ($N > 2$). Our conclusions strictly hold only for the analytic P_L acceleration methods. However, previous experience with the DSA method has shown that our results are indicative for the associated discretized versions of P_L accelerations, in particular, if the differencing of the synthetic equations is consistent with that of the transport equation.[4-6]

ACKNOWLEDGMENTS

Work by one of the authors (DV) was supported in part by U.S. Department of Energy Grant DE-AS05-80ER10711 and National Science Foundation Grant DMS-8312451.

REFERENCES

1. H. J. KOPP, *Nucl. Sci. Eng.*, **17**, 65 (1963).

2. E. M. GELBARD and I. A. HAGEMAN, *Nucl. Sci. Eng.*, **37**, 288 (1969).

3. W. H. REED, *Nucl. Sci. Eng.*, **45**, 245 (1971).

4. R. E. ALCOUFFE, *Nucl. Sci. Eng.*, **64**, 344 (1977).

5. E. W. LARSEN, *Nucl. Sci. Eng.*, **82**, 47 (1982).

6. E. W. LARSEN, *TTSP*, **13**, 107 (1984).

7. W. F. MILLER and E. W. LARSEN, *Nucl. Sci. Eng.*, **93**, 403 (1986).

8. J. E. MOREL, *Nucl. Sci. Eng.*, **82**, 34 (1982).

9. M. WILLIAMS, *TTSP*, **13**, 127 (1984).

10. W. F. MILLER, Jr., *Nucl. Sci. Eng.*, **65**, 226 (1978).